Supplementary Materials for

Sensitive Real-Time Monitoring of Refractive Indexes Using a Novel Graphene-Based Optical Sensor

Fei Xing,[1] Zhi-Bo Liu,[1,] Zhi-Chao Deng,[1] Xiang-Tian Kong,[1] Xiao-Qing Yan,[1,2] Xu-Dong Chen,[1] Qing Ye,[1] Chun-Ping Zhang,[1] Yong-Sheng Chen[2], & Jian-Guo Tian[1,]

1 The Key Laboratory of Weak Light Nonlinear Photonics, Ministry of Education, Teda Applied Physics School and School of Physics, Nankai University, Tianjin 300071, China
2 The Key Laboratory of Functional Polymer Materials and Center for Nanoscale Science & Technology, Institute of Polymer Chemistry, College of Chemistry, Nankai University, Tianjin 300071, China

This file includes:

Theory of total internal reflection

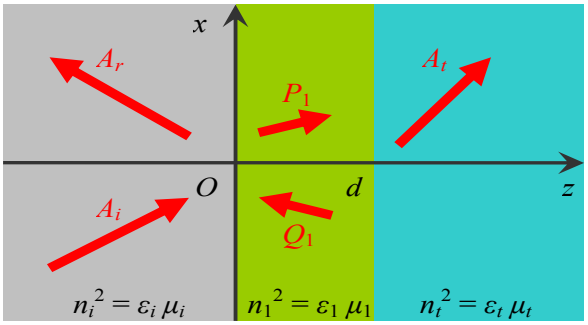

Fig. S1. Schematic graph of tri-layered structure. The relative permittivity (ε) and permeability (μ) are shown in each layer.

The concerned structure is shown in Fig. S1. The plane of incidence is assumed to be *x*, *z*-plane, and both the boundaries are perpendicular to z axis. Maxwell equations remain unchanged when E and H and simultaneously ε and $-\mu$ are interchanged. Thus the theorem for transverse magnetic (TM) waves can be immediately deduced from the corresponding result for transverse electric (TE) waves. For TE waves, $E_x, E_z, H_y = 0$ and $\partial / \partial y = 0$, Maxwell equations deduced to (time dependence $\exp(-i\omega t)$ being assumed) (Fig. S1)

$$\begin{aligned} \frac{\partial H_x}{\partial z} - \frac{\partial H_z}{\partial z} + i\omega\varepsilon E_y &= 0, \\ \frac{\partial E_y}{\partial z} + i\omega\mu H_x &= 0, \\ \frac{\partial E_y}{\partial x} - i\omega\mu H_z &= 0. \end{aligned} \tag{1}$$

In each layer, the fields can be written as superpositions of positive- and negative-going secondary waves. Thus, E_y is given by

$$E_y = \begin{cases} (A_i e^{ik_{iz}z} + A_r e^{-ik_{iz}z}) e^{ik_x x}, & z \le 0, \\ (P_1 e^{ik_{1z}z} + Q_1 e^{-ik_{1z}(z-d)}) e^{ik_x x}, & 0 \le z \le d, \\ A_t e^{ik_{tz}(z-d)} e^{ik_x x}, & z \ge d. \end{cases} \tag{2}$$

Here $k_{iz} = n_i k_{0z}$, $k_{1z} = n_1 k_{0z}$, $k_{tz} = n_t k_{0z}$, and $k_x = n_i k_{0x}$, where k_0 is free space wavevector and $n = \sqrt{\varepsilon_r \mu_r}$ is refractive index, ε_r and μ_r being relative permittivity and relative permeability respectively (Fig. s1). A_i, A_r, and A_t are defined as incident, reflected and transmitted amplitude coefficient. As a result of the boundary

condition, x component of wavevector of all the layers is equal to each other. According to Eqs. (1) and (2), the magnetic components are given by

$$H_x = \begin{cases} -\dfrac{k_{iz}}{\omega\mu_0\mu_i}(A_i e^{ik_{iz}z} - A_r e^{-ik_{iz}z})e^{ik_x x}, & z \le 0, \\ -\dfrac{k_{1z}}{\omega\mu_0\mu_1}(P_1 e^{ik_{1z}z} - Q_1 e^{-ik_{1z}(z-d)})e^{ik_x x}, & 0 \le z \le d, \\ -\dfrac{k_{tz}}{\omega\mu_0\mu_t} A_t e^{ik_{tz}(z-d)} e^{ik_x x}, & z \ge d; \end{cases} \tag{3}$$

and

$$H_z = \frac{kx}{\omega\mu} E_y. \tag{4}$$

By applying the boundary condition of the continuities of E_y and H_x, we have:

$$\begin{bmatrix} A_i \\ A_r \end{bmatrix} = \frac{1}{2}\begin{bmatrix} 1+\dfrac{k_{1z}}{k_{iz}}\gamma_{i1} & (1-\dfrac{k_{1z}}{k_{iz}}\gamma_{i1})e^{ik_{1z}d} \\ 1-\dfrac{k_{1z}}{k_{iz}}\gamma_{i1} & (1+\dfrac{k_{1z}}{k_{iz}}\gamma_{i1})e^{ik_{1z}d} \end{bmatrix}\begin{bmatrix} P_1 \\ Q_1 \end{bmatrix} \tag{5}$$

$$\begin{bmatrix} P_1 \\ Q_1 \end{bmatrix} = \frac{1}{2}\begin{bmatrix} (1+\dfrac{k_{tz}}{k_{1z}}\gamma_{1t})e^{-ik_{1z}d} \\ 1-\dfrac{k_{tz}}{k_{1z}}\gamma_{1t} \end{bmatrix} A_t. \tag{6}$$

Here, $\gamma_{i1} = \mu_i / \mu_1$ and $\gamma_{1t} = \mu_1 / \mu_t$. Thus, the relation between A_i, A_r and A_t can be written as

$$\begin{bmatrix} A_i \\ A_r \end{bmatrix} = \mathbf{M} A_t, \tag{7}$$

where

$$\mathbf{M} = \frac{1}{4}\begin{bmatrix} 1+\dfrac{k_{1z}}{k_{iz}}\gamma_{i1} & (1-\dfrac{k_{1z}}{k_{iz}}\gamma_{i1})e^{ik_{1z}d} \\ 1-\dfrac{k_{1z}}{k_{iz}}\gamma_{i1} & (1+\dfrac{k_{1z}}{k_{iz}}\gamma_{i1})e^{ik_{1z}d} \end{bmatrix}\begin{bmatrix} (1+\dfrac{k_{tz}}{k_{1z}}\gamma_{1t})e^{-ik_{1z}d} \\ 1-\dfrac{k_{tz}}{k_{1z}}\gamma_{1t} \end{bmatrix}. \tag{8}$$

For TM waves, the relations between amplitude coefficients are all the same as those for TE waves, expect that the parameters γ_{i1} and γ_{1t} are defined by $\gamma_{i1} = \varepsilon_i / \varepsilon_1$ and $\gamma_{1t} = \varepsilon_1 / \varepsilon_t$. For nonmagnetic materials, the relative permeability is equal to one, so for TE

waves, $\gamma_{i1} = \gamma_{1t} = 1$, and for TM waves, $\gamma_{i1} = n_i^2 / n_1^2$ and $\gamma_{1t} = n_1^2 / n_t^2$.

In particular, if $d = 0$, the structure reduces to two semi-infinite materials bounded by $z = 0$. Thus $P_1 = A_t$, $Q_1 = 0$. So we have

$$\mathbf{M} = \frac{1}{2}\begin{bmatrix} 1 + \dfrac{k_{tz}}{k_{iz}}\gamma_{it} \\ 1 - \dfrac{k_{tz}}{k_{iz}}\gamma_{it} \end{bmatrix}, \tag{9}$$

where γ_{it} is equal to μ_i / μ_t for TE waves, and $\varepsilon_i / \varepsilon_t$ for TM waves. It is noted that Eq. (9) is consistent with Fresnel formulae.

$\mathbf{M}$ is a 2×1 matrix, whose elements are denoted by M_1 and M_2, respectively. Thus we have $A_r = \dfrac{M_2}{M_1} A_i$ and $A_t = A_i / M_1$. The light intensity is given by the amplitude of Poynting vector

$$S = |\mathbf{E} \times \mathbf{H}| = \sqrt{\varepsilon / \mu} E^2 = \sqrt{\mu / \varepsilon} H^2. \tag{10}$$

For TE waves, the amount of energy that is incident on a unit area of the boundary ($z = 0$) per second is given by

$$J_i = S_{iz} = \sqrt{\frac{\varepsilon_0 \varepsilon_i}{\mu_0 \mu_i}} \frac{k_{iz}}{n_i k_0} |A_i|^2 . \tag{11}$$

Similarly, the energies that are reflected and transmitted from unit areas of the boundaries ($z = 0$ and $z = d$) per second are given by

$$J_r = S_{rz} = \sqrt{\frac{\varepsilon_0 \varepsilon_i}{\mu_0 \mu_i}} \frac{k_{iz}}{n_i k_0} |A_r|^2, \tag{12}$$

$$J_t = S_{tz} = \sqrt{\frac{\varepsilon_0 \varepsilon_t}{\mu_0 \mu_t}} \frac{\mathrm{Re}(k_{tz})}{n_t k_0} |A_t|^2 . \tag{13}$$

Therefore, the reflectance R and transmittance T are given by

$$R = \frac{J_r}{J_i} = \left|\frac{A_r}{A_i}\right|^2 = \frac{M_2 M_2^*}{M_1 M_1^*}, \tag{14}$$

$$T = \frac{J_t}{J_i} = \frac{\mu_i}{\mu_t} \frac{\mathrm{Re}(k_{tz})}{k_{iz}} \left|\frac{A_t}{A_i}\right| = \frac{\mu_i}{\mu_t} \frac{\mathrm{Re}(k_{tz})}{k_{iz}} \frac{1}{M_1 M_1^*}. \tag{15}$$

For TM waves, the reflectance and transmittance can be immediately known by interchanging ε and $^{-}\mu$ in Eqs. (14) and (15). We find that R for TM waves is the same as that for TE waves (Eq. (14)), whereas for TM waves,

$$T = \frac{\varepsilon_i}{\varepsilon_t}\frac{\mathrm{Re}(k_{tz})}{k_{iz}}\left|\frac{A_t}{A_i}\right| = \frac{\varepsilon_i}{\varepsilon_t}\frac{\mathrm{Re}(k_{tz})}{k_{iz}}\frac{1}{M_1 M_1^*}. \tag{16}$$

It can be proved that $R+T=1$ for lossless materials, which means energy conservation of the waves.

Energy density of the electromagnetic field is defined by $W = W_e + W_m$, where $W_e = \frac{1}{2}\mathbf{E}\cdot\mathbf{D}$ and $W_m = \frac{1}{2}\mathbf{H}\cdot\mathbf{B}$ are electric energy density and magnetic energy density, respectively.

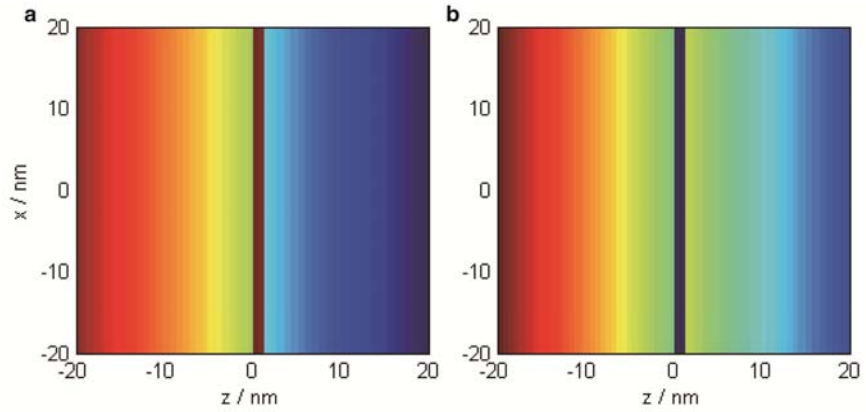

Fig. S2. Energy density distributions of a four-layer graphene. (**a** to **b**) Energy density distributions of a four-layer graphene (d = 1.36 nm, $n_1 = n' = 2.6 + 1.6\mathrm{i}$) sandwiched between two semi-infinite mediums (n_i = 1.61 and n_t = 1.41) under 633 nm illumination with incident angle θ = 75 degrees. **a**: TE; **b**: TM. The incident energy densities of TE and TM waves are normalized equal. A, B are plotted with the same color sale.

For a system consisting a four-layer graphene (d = 1.36 nm, $n_1 = n' = 2.6 + 1.6\mathrm{i}$) sandwiched between two semi-infinite mediums (n_i = 1.61 and n_t = 1.41), the energy density is shown in Fig. S2a and S2b, for TE and TM waves, respectively. Apparently, the graphene layer stores more energy for TE waves than for TM waves. In Figs. S2a and b, the energy densities of incident waves are normalized equal.

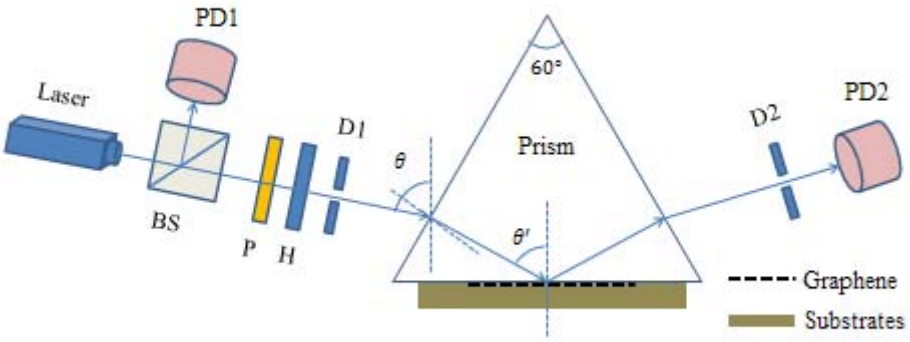

Fig. S3. Schematic of the derivative total reflection method setup. BS, beam splitter; P, polarizer; H, half wavelength plate; PD1, PD2, photodetector; D1, D2, aperture; θ is the incident angle and has a relation with θ' as $\sin(\theta\text{-}60°)=n\times\sin(\theta'\text{-}60°)$, where n is the refractive index of prism.

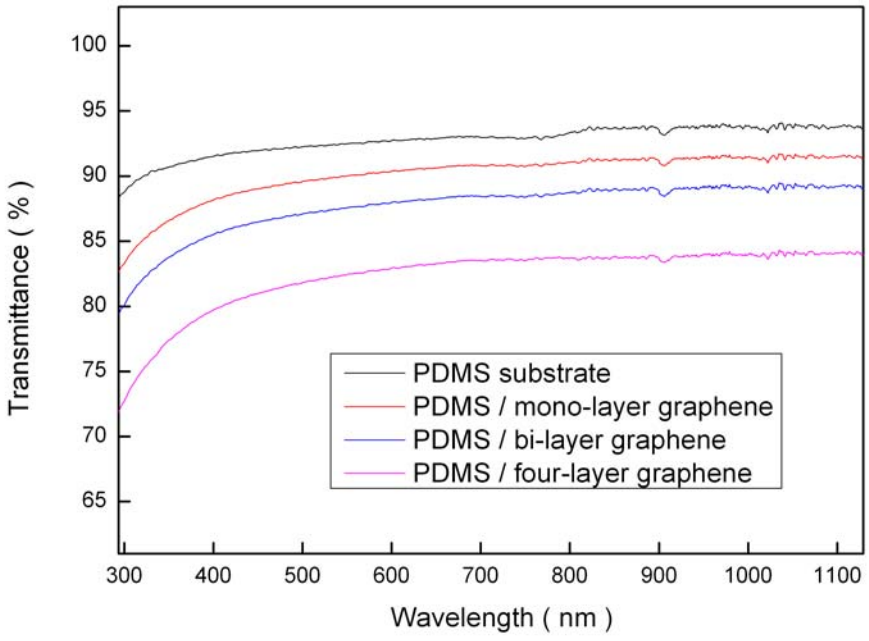

Fig. S4. Optical transmittance of the graphene samples with different number of layers. The absorbance of graphene sample used in the experiment is about 9% in a broad wavelength range.

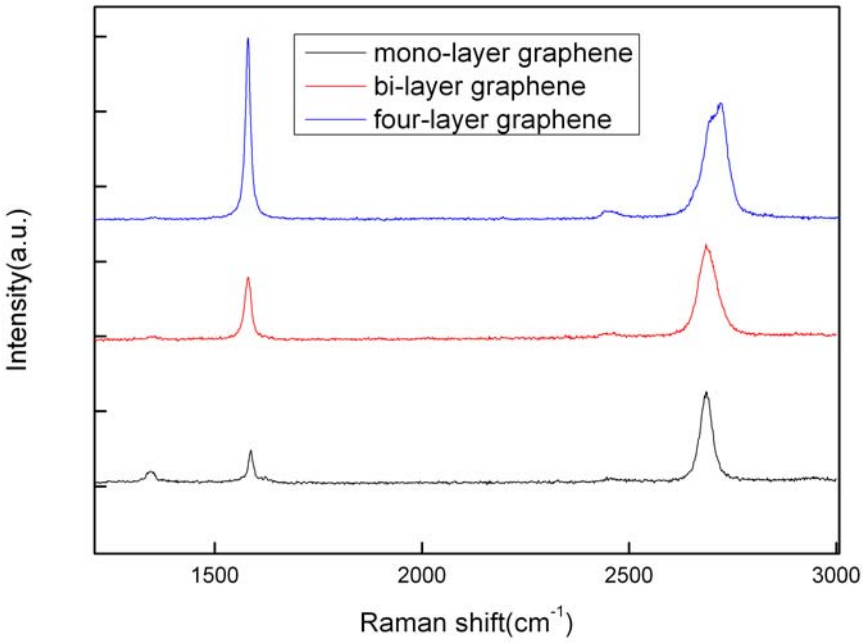

Fig. S5. The Raman spectrum of multi-layer graphene.

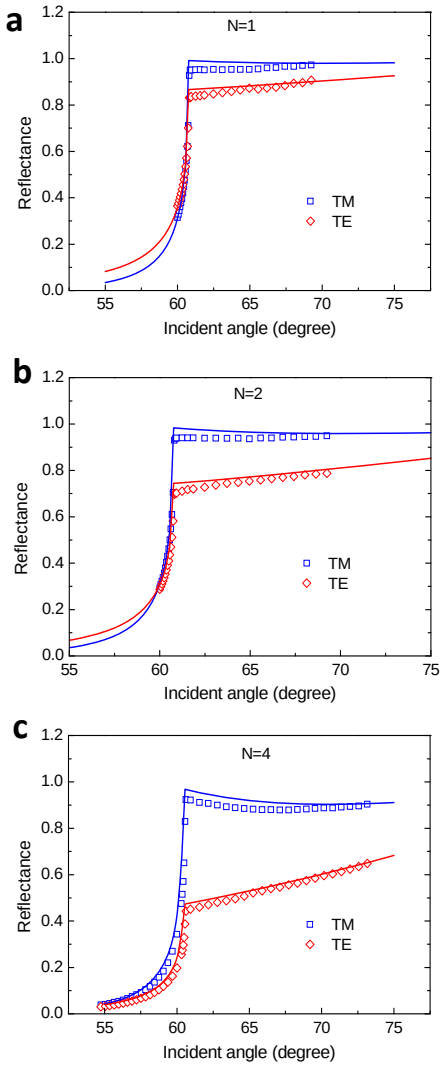

Fig. S6. Experimental and calculated angular dependence of optical reflectance of *p*- to *s*-polarized light for (a) Monolayer graphene (N=1), (b) Bilayer graphene (N=2), (c) Four-layer graphene (N=4) with $n = 2.6$ and $\kappa = 1.6$.

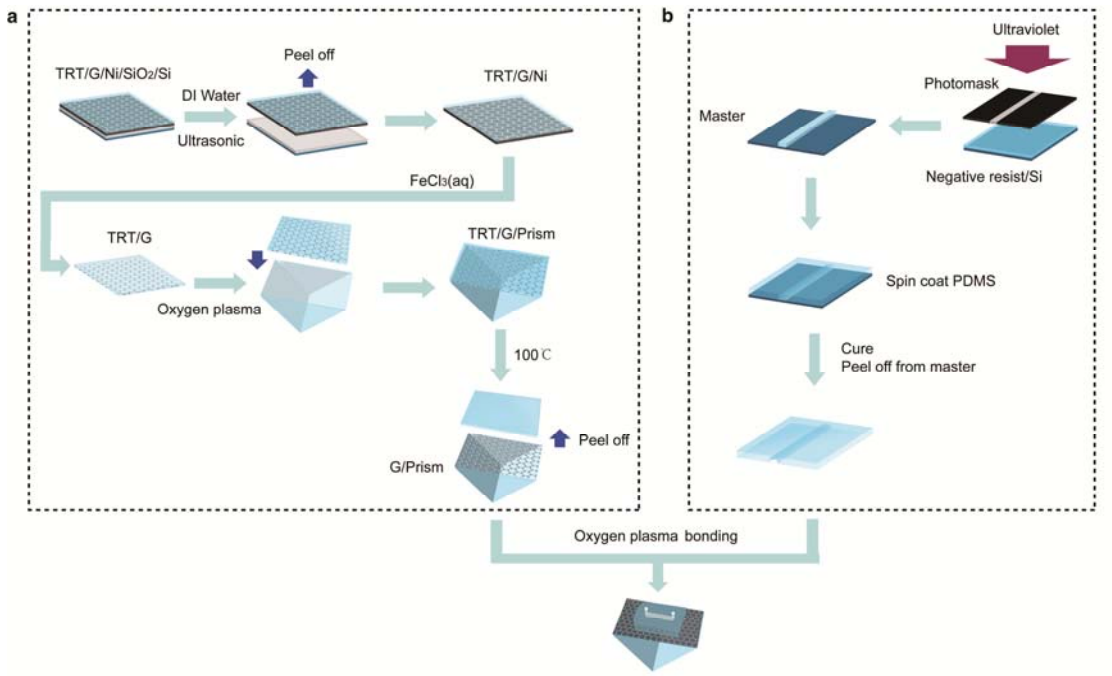

Fig. S7. Schematic of preparing the GRIS with microfluid chanel.

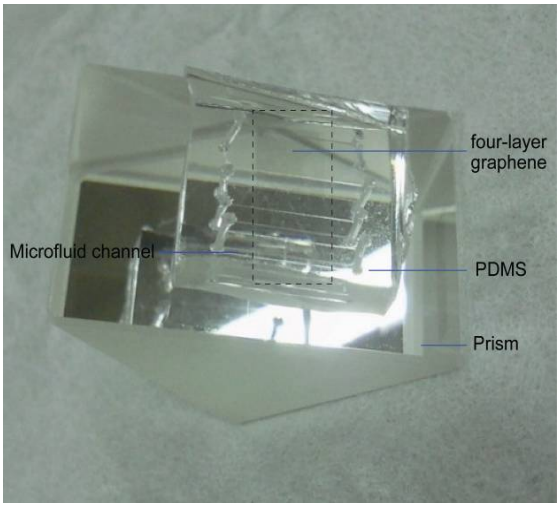

Fig. S8. The real diagram of GRIS with microfluid chanel.

Table. S1. The list of refractive indexes of NaCl solution of different weight percentage of concentration.

Concentration of NaCl solution (%)	Refractive index
0	1.33091
0.1	1.33139
1	1.33263
2	1.33457
5	1.33961
10	1.34794
15	1.35715
20	1.36670
25	1.37539

Table. S2. The list of refractive indexes of glucose solution of different weight percentage of concentration.

Concentration of glucose solution (%)	Refractive index
0	1.33091
1	1.33192
2	1.33367
5	1.33713
10	1.34308
15	1.34911
20	1.35574
25	1.36203